present study demonstrates a 2-D shadow image of the 3-D onion-like SW structure. Consequently, the aforementioned difference in the reduction of the SW does not provide a real 3-D reduction in SWs in the human skull. Note that the reduction effect of the SW by the random modulation method cannot be assumed to actually increase in the human skull bone (Fig. 8).

Although the values of R_{SW} are lower for random modulation methods than for sinusoidal activation in the human skull, the degree of the reduction in R_{SW} is smaller compared with the reflective plate case (*e.g.*, rR_{SW} = 9.6 [plate, ROI A], whereas rR_{SW} = 5.0 [skull] in the case of RSBIC activation). The reason for this might be explained as follows. Because the randomly modulated wave already has a kind of distorted waveform in the traveling wave, the spatial distortion is not increased by the reflection at the curved surface of the human skull. Phenomenologically, the spatial distortion level of the SW is not expected to increase further.

The random modulation method treated in the present study appears to have a high potential for avoiding a fundamental adverse effect in various transcranial ultrasonic therapeutic techniques, such as tumor ablation by transcranial HIFU, open BBB in drug delivery systems, rapid recanalization in acute ischemic stroke and neurologic stimulation of the central nervous system. An application for actual transcranial sonotherapy is strongly anticipated in order to implement various therapeutic equipment for preventing brain tissue damage due to SWs.

Acknowledgments—This work was supported by a Grant for Research on Advanced Technology (H21-008) from the Ministry of Health, Labor, and Welfare of Japan. The authors thank Dr. Jun Shimizu for cutting the human skull bone to be suitable for the present study and Nami Saito for technical assistance.

REFERENCES

Ammi AY, Mast TD, Huang IH, Abruzzo TA, Coussios CC, Shaw GJ, Holland CK. Characterization of ultrasound propagation through ex vivo human temporal bone. Ultrasound Med Biol 2008;34:1578–1589.

Azuma T, Kawabata K, Umemura S, Ogihara M, Kubota J, Sasaki A, Furuhata H. Schlieren observation of therapeutic field in water surrounded by cranium radiated from 500 kHz ultrasonic sector transducer. Proc IEEE Ultrason Symp 2004;2:1001–1004.

Azuma T, Kawabata K, Umemura S, Ogihara M, Kubotal J, Sasaki A, Furuhata H. Bubble generation by standing wave in water surrounded by cranium with transcranial ultrasonic beam. Jpn J Appl Phys 2005;4625–4630.

Azuma T, Ogihara M, Kubota J, Sasaki A, Umemura S, Furuhata H. Dual-frequency ultrasound imaging and therapeutic bilaminar array using frequency selective isolation layer. IEEE trans Ultrason Ferroelectr Freq Control 2010;57:1211–1224.

Baron C, Aubry JF, Tanter M, Meairs S, Fink M. Simulation of intracranial acoustic fields in clinical trials of sonothrombolysis. Ultrasound Med Biol 2009;35:1148–1158.

Chapelon JY, Dupenloup F, Cohen H, Lentz P. Reduction of cavitation using pseudorandom signals [therapeutic US]. IEEE Trans Ultrason Ferroelectr Freq Control 1996;43:623–625.

Clement GT, White PJ, King RL, McDannold N, Hynynen K. A magnetic resonance imaging-compatible, large-scale array for trans-skull ultrasound surgery and therapy. J Ultrasound Med 2005;24:1117–1125.

Culp WC, McCowan TC. Ultrasound augmented thrombolysis. Current Med Imaging Reviews 2005;1:5–12.

Daffertshofer M, Fatar M. Therapeutic ultrasound in ischemic stroke treatment: Experiment evidence. Eur J Ultrasound 2002;16:121–130.

Daffertshofer M, Gass A, Ringleb P, Sitzer M, Sliwka U, Els T, Sedlaczek O, Koroshetz WJ, Hennerici MG. Transcranial low-frequency ultrasound-mediated thrombolysis in brain ischemia: increased risk of hemorrhage with combined ultrasound and tissue plasminogen activator: results of a phase II clinical trial. Stroke 2005;36:1441–1446.

Deffieux T, Konofagou EE. Numerical study of a simple transcranial focused ultrasound system applied to blood-brain barrier opening. IEEE Trans Ultrason Ferroelectr Freq Control 2010;57:2637–2653.

Fry WJ. Ultrasound in neurology. Neurology 1956;6:693–704.

Fry WJ, Fry FJ. Fundamental neurological research and human neurosurgery using intense ultrasound. IRE Trans Med Electron 1960;ME-7:166–181.

Fry FJ, Goss SA, Patrick JT. Transkull focal lesions in cat brain produced by ultrasound. J Neurosurg 1981;54:659–663.

Hynynen K, Clement G. Clinical applications of focused ultrasound - the brain. Int J Hyperthermia 2007;23:193–202.

Hynynen K, McDannold N, Clement G, Jolesz FA, Zadicario E, Killiany R, Moore T, Rosen D. Preclinical testing of a phased array ultrasound system for MRI-guided noninvasive surgery of the brain: A primate study. Eur J Radiology 2006;59:149–156.

Hynynen K, McDannold N, Vykhodtseva N, Jolesz FA. Noninvasive MR imaging-guided focal opening of the blood-brain barrier in rabbits. Radiology 2001;220:640–646.

Hynynen K, McDannold N, Vykhodsteva N, Raymond S, Weissleder R, Jolesz FA, Sheikov N. Focal disruption of the blood-brain barrier due to 260-kHz ultrasound bursts: a method for molecular imaging and targeted drug delivery. J Neurosurg 2006;105:445–454.

Kawata H, Naya N, Takemoto Y, Uemura S, Nakajima T, Horii M, Takeda Y, Fujimoto S, Yamashita A, Asada Y, Saito Y. Ultrasound accelerates thrombolysis of acutely induced platelet-rich thrombi similar to those in acute myocardial infarction. Circ J 2007;71:1643–1648.

Konofagou EE, Tung YS, Choi J, Deffieux T, Baseri B, Vlachos F. Ultrasound-induced blood-brain barrier opening. Curr Pharm Biotechnol 2012;13:1332–1345.

Kuroiwa Y, Yamashita A, Miyati T, Furukoji E, Takahashi M, Azuma T, Sugimura H, Asanuma T, Tamura S, Kawai K, Asada Y. MR signal change in venous thrombus relates organizing process and thrombolytic response in rabbit. Magn Reson Imaging 2011;29:975–984.

Marsac L, Chauvet D, Larrat B, Pernot M, Robert B, Fink M, Boch AL, Aubry JF, Tanter M. MR-guided adaptive focusing of therapeutic ultrasound beams in the human head. Med Phys 2012;39:1141–1149.

McDannold N, Park EJ, Mei CS, Zadicario E, Jolesz F. Evaluation of three-dimensional temperature distributions produced by a low-frequency transcranial focused ultrasound system within ex vivo human skulls. IEEE Trans Ultrason Ferroelectr Freq Control 2010;57:1967–1976.

Mikulik R, Alexandrov AV. Acute stroke: Therapeutic transcranial Doppler sonography. Front Neurol Neurosci 2006;21:150–161.

Miyata S, Kawabata S, Hiramatsu R, Doi A, Ikeda N, Yamashita T, Kuroiwa T, Kasaoka S, Maruyama K, Miyatake S. Computed tomography imaging of transferrin targeting liposomes encapsulating both boron and iodine contrast

agents by convection-enhanced delivery to F98 rat glioma for boron neutron capture therapy. Neurosurgery 2011;68:1380–1387 discussion 1387.

Pinton G, Aubry JF, Fink M, Tanter M. Numerical prediction of frequency dependent 3D maps of mechanical index thresholds in ultrasonic brain therapy. Med Phys 2012;3981:455–467.

Song J, Pulkkinen A, Huang Y, Hynynen K. Investigation of standing-wave formation in a human skull for a clinical prototype of a large-aperture, transcranial MR-guided focused ultrasound (MRgFUS) phased array: An experimental and simulation study. IEEE Trans Biomed Eng 2012;59:435–444.

Shimizu J, Fukuda T, Abe T, Ogihara M, Kubota J, Sasaki A, Azuma T, Sasaki K, Shimizu K, Oishi T, Umemura S, Furuhata H. Ultrasound safety with midfrequency transcranial sonothrombolysis: preliminary study on normal macaca monkey brain. Ultrasound Med Biol 2012;38:1040–1050.

Tang SC, Clement GT. Standing wave suppression for transcranial ultrasound by random-modulation. IEEE Trans Biomed Eng 2010;57:203–205.

Tang SC, Clement GT. Acoustic standing wave suppression using randomized phase-shift-keying excitations. J Acoust Soc Am 2009;126:1667–1670.

Journal of the Neurological Sciences 323 (2012) 99–103

Contents lists available at SciVerse ScienceDirect

Journal of the Neurological Sciences

journal homepage: www.elsevier.com/locate/jns

Low DWI-ASPECTS is associated with atrial fibrillation in acute stroke with the middle cerebral artery trunk occlusion

Yuki Sakamoto [a], Masatoshi Koga [b], Kazunori Toyoda [a,*], Masato Osaki [a], Takuya Okata [a], Kazuyuki Nagatsuka [c], Kazuo Minematsu [a]

[a] Department of Cerebrovascular Medicine, National Cerebral and Cardiovascular Center, Suita, Japan
[b] Division of Stroke Care Unit, National Cerebral and Cardiovascular Center, Suita, Japan
[c] Department of Neurology, National Cerebral and Cardiovascular Center, Suita, Japan

ARTICLE INFO

Article history:
Received 22 May 2012
Received in revised form 20 August 2012
Accepted 29 August 2012
Available online 27 September 2012

Keywords:
Acute ischemic stroke
Diffusion-weighted imaging
Atrial fibrillation

ABSTRACT

Background and purpose: For optimal acute stroke management and secondary prevention, discrimination of stroke etiology is crucial. We hypothesized that a low Alberta Stroke Program Early CT Score (ASPECTS) on diffusion-weighted imaging (DWI) immediately after stroke onset was associated with the presence of atrial fibrillation (AF).

Methods: Consecutive patients admitted within 24 h from stroke onset with an occlusion at the horizontal segment of the middle cerebral artery (M1) on initial MRA were retrospectively enrolled. AF was diagnosed based on continuous electrocardiogram monitoring during acute hospitalization or its confirmed history.

Results: Of the 206 patients (95 women, median age 77 [IQR 69–85] years, NIHSS score 18 [13–23]) enrolled, AF was identified in 138 patients (AF group): chronic AF in 89, known paroxysmal AF (pAF) in 13, and masked pAF on admission in 36. The ASPECTS score on the initial DWI, performed a median of 2.5 h after onset, was lower in the AF group than in the others (4 [2–6] vs. 7 [4–8], $p<0.001$). With the optimal cut-off value of ≤6 (sensitivity, 78%; specificity, 57%; area under the ROC curve, 0.682), DWI-ASPECTS was independently associated with the presence of any AF (OR 5.05, 95%CI 2.36 to 10.8), as well as the presence of any pAF (OR 8.64, 95%CI 3.00 to 24.9) and that of masked pAF on admission (OR 10.0, 95%CI 3.06 to 32.9).

Conclusion: Extensive early ischemic change assessed by DWI-ASPECTS predicts the presence of AF, even initially masked pAF, in acute stroke patients with M1 occlusion.

1. Introduction

The etiological mechanisms of cardioembolic stroke differ from those of other ischemic strokes, and accordingly, there are unique strategies for acute management and secondary prevention, including urgent anticoagulant therapy and rapid exploration for cardiac thrombi. Thus, prompt diagnosis of cardioembolic stroke is crucial, especially in the hyperacute phase. However, detection of atrial fibrillation (AF), the leading cause of cardioembolic stroke, is often difficult due to the existence of paroxysmal AF (pAF) [1].

Diffusion-weighted magnetic resonance imaging (DWI, MRI) depicts ischemic lesions clearly [2]. Combined with magnetic resonance angiography (MRA), DWI contributes to rapid and accurate diagnosis of ischemic stroke subtype [3]. Although the presence of atherosclerotic changes of the responsible artery on MRA is a good indicator to distinguish atherothrombotic infarction from cardioembolism [3], this information is not available when MRA reveals complete arterial occlusion. Large infarct volume is another promising factor to distinguish cardioembolic infarcts with high-risk embolic sources from infarcts with internal carotid artery (ICA) atherosclerosis [4], and it is applicable to patients with arterial occlusion. The Alberta Stroke Program Early CT Score (ASPECTS) on DWI is a semi-quantitative topographic score that can simply estimate the extent of infarct area immediately after stroke [5,6], and it has been proven to correlate inversely with DWI lesion volume [7,8]. The aim of this study was to examine the hypothesis that acute stroke patients with occlusion at the horizontal segment (M1) of the middle cerebral artery (MCA) who had AF had lower DWI-ASPECTS scores than those without AF.

2. Methods

2.1. Subjects

Consecutive acute ischemic stroke patients who underwent MRI/MRA on admission to our stroke center within 24 h from stroke onset from April 2006 through August 2011 and were diagnosed as having

* Corresponding author at: Department of Cerebrovascular Medicine, National Cerebral and Cardiovascular Center, 5-7-1 Fujishiro-dai, Suita, Osaka 565-8565, Japan. Tel.: +81 6 6833 5012; fax: +81 6 6835 5267.
E-mail address: toyoda@hsp.ncvc.go.jp (K. Toyoda).

0022-510X/$ – see front matter © 2012 Elsevier B.V. All rights reserved.
http://dx.doi.org/10.1016/j.jns.2012.08.021

M1 occlusion with compatible acute neurological deficits were retrospectively enrolled. Patients with contraindications to MRI were excluded.

This study was approved by the institutional ethics committee.

2.2. Clinical backgrounds and characteristics

Clinical backgrounds, including sex, age, and cardiovascular risk factors, were reviewed. Cardiovascular risk factors were defined as: 1) hypertension, history of using antihypertensive agents, systolic blood pressure ≥140 mm Hg, or diastolic blood pressure ≥90 mm Hg before or ≥2 weeks after stroke onset; 2) diabetes mellitus, use of hypoglycemic agents, random glucose level ≥200 mg/dl, or glycosylated hemoglobin ≥6.5% on admission; 3) hyperlipidemia, use of antihyperlipidemic agents, or a serum total cholesterol level ≥220 mg/dl; and 4) current smoking and alcohol intake. Stroke severity was assessed using the National Institutes of Health Stroke Scale (NIHSS).

2.3. Identification of atrial fibrillation

For detecting AF, a 12-lead electrocardiogram (ECG) on admission and continuous ECG monitoring for the initial several days of hospitalization (at least 24 h) were conducted in all patients. These examinations were repeated during acute hospitalization when patients were suspected to have AF based on complaints of palpitations. Patients with AF (the AF group) were classified into three subgroups: those with chronic AF (cAF), those with known paroxysmal AF (pAF) as a confirmed history or identification on the initial ECG, and those with masked pAF on admission that was later identified. Patients who did not have a history of AF or in whom AF was not detected on ECG were defined as the non-AF group.

2.4. Neuroimaging

MRI studies including DWI and MRA were performed on admission using a commercially available echo planar instrument operating at 1.5 T (Siemens MAGNETOM Vision or MAGNETOM Sonata scanner, Erlangen, Germany). DWI was obtained using the following parameters: TR/TE, 4000/100 ms; b values, 0 and 1000 s/mm^2; field of view, 24 cm; acquisition matrix, 96×128; and slice thickness, 4.0 mm, with a 1.0-mm intersection gap.

DWI-ASPECTS was scored by a neurologist (Y.S.) who was blinded to all clinical information, based on the method described by Barber et al. [5]. The MCA territory was allotted 10 points, and a single point was subtracted for an area of hyperintensity on initial DWI. A score of 0 indicated complete ischemic involvement throughout the MCA territory. The inter-rater reliability of DWI-ASPECTS was evaluated using scores by another neurologist (T.O.) with weighted κ statistics. The intra-rater reliability was examined with scores recorded after a 2-month interval from the initial evaluation by the same neurologist (Y.S.). The site of arterial occlusion was determined on the initial MRA. M1 occlusion was judged irrespective of the presence of ipsilateral ICA occlusion. Patients with the horizontal distance from the ICA bifurcation to the distal end of the flow signal at M1 in an anteroposterior view <5 mm were defined as having M1 proximal occlusion, while those in whom this residual vessel length was ≥5 mm were defined as having M1 distal occlusion [9].

2.5. Statistical analysis

Clinical backgrounds and characteristics were compared between the AF and non-AF groups. Univariate analyses were performed using the chi-square test, Fisher's exact test, or the Mann–Whitney U test as appropriate. The data are presented as median values (interquartile range [IQR]) or frequencies (%). To obtain the optimal cut-off value of DWI-ASPECTS for discriminating the AF group from the non-AF group, receiver-operating characteristic (ROC) curve analysis was conducted. Multivariate logistic regression analyses were performed to identify independent factors associated with the presence of AF. DWI-ASPECTS and all variables of clinical manifestations identified on univariate analyses with p values <0.1 were entered into the model. Multivariate analyses were also performed to identify factors related to the presence of pAF after removing patients with cAF from the cohort, while factors related to the presence of masked pAF were identified after removing patients with cAF and those with known pAF.

All statistical analyses were performed using PASW for Windows version 17.0 software (SPSS Inc., Chicago, IL, USA). Results were considered significant at $p<0.05$.

3. Results

Overall, 1461 patients with acute ischemic stroke were admitted to our stroke center during the study period (Fig. 1). Of these, 123 patients were excluded due to: MRI contraindicated in 105; missing the MRA sequence on the initial MR examination in 12; and difficult evaluation of the imaging due to motion artifact in 6. Of the remaining 1338 patients, arterial occlusion at M1 was observed in 206 patients. Finally, these 206 patients (95 women, median age 77 [IQR 69–85] years, NIHSS score 18 [13–23]) were enrolled in the present study.

AF was observed in 138 patients (AF group), while it was not observed in the remaining 68 patients (non-AF group). In the AF group, 89 (65%) patients had cAF, 13 (9%) had known pAF, and the remaining 36 (26%) had masked pAF. The clinical characteristics of the included patients are presented in Table 1. Patients in the AF group were older ($p<0.001$) and had a higher NIHSS score ($p=0.004$) than those in the non-AF group. Male sex ($p=0.037$), hyperlipidemia ($p=0.005$), and current smoking ($p=0.001$) were less common, and the plasma D-dimer ($p=0.029$) level was higher in the AF group than in the non-AF group.

The initial MRI was performed a median 2.5 h (IQR 1.5–8.2 h) after stroke onset. Overall, 121 patients (59%) had M1 proximal occlusion. The DWI-ASPECTS was significantly lower in the AF group than in the non-AF group (median 4 [IQR 2–6] vs. 7 [4–8], $p<0.001$, Table 1). The inter-rater reliability of DWI-ASPECTS was $\kappa=0.69$, and intra-rater reliability was $\kappa=0.72$. The proportion of patients with AF decreased along with the increase in DWI-ASPCETS ($r=-0.843$, $p=0.001$ with Spearman's rank correlation test, Fig. 2). Using the ROC curve, the optimal cut-off value of DWI-ASPECTS distinguishing the AF group from the non-AF group was ≤6 (sensitivity, 78%; specificity, 57%; area under the ROC curve, 0.682).

The results of multivariate regression analysis for association with AF are presented in Table 2. DWI-ASPECTS ≤6 (OR 5.05, 95%CI 2.36 to 10.8, $p<0.001$) and advanced age (OR 1.47, 95%CI 1.03 to 2.09, $p=0.034$ for every 10 years) were positively associated, and hyperlipidemia (OR 0.48, 95%CI 0.24 to 0.99, $p=0.047$) and current smoking (OR 0.31, 95%CI 0.13 to 0.73, $p=0.007$) were inversely associated with having AF. DWI-ASPECTS ≤6 was associated with having AF when the analysis was done only for patients with M1 proximal occlusion (OR 6.92, 95%CI 2.11 to 22.7, $p=0.001$) and only for those with M1 distal occlusion (OR 6.95, 95%CI 1.96 to 24.6, $p=0.003$). DWI-ASPECTS was also associated with having AF as a continuous variable (OR 0.76, 95%CI 0.65 to 0.88 for every 1 point).

The results of multivariate analyses for association with pAF are presented in Table 3. DWI-ASPECTS ≤6 was positively associated with the presence of any pAF (both known and masked pAF, OR 8.64, 95%CI 3.00 to 24.9) and with the presence of masked pAF (OR 10.0, 95%CI 3.06 to 32.9).

4. Discussion

In the present study, a significant association between the initial DWI-ASPECTS and the presence of AF was demonstrated in acute ischemic stroke patients with M1 occlusion. DWI-ASPECTS of 6 or less could predict AF irrespective of the M1 occlusion site. Moreover,

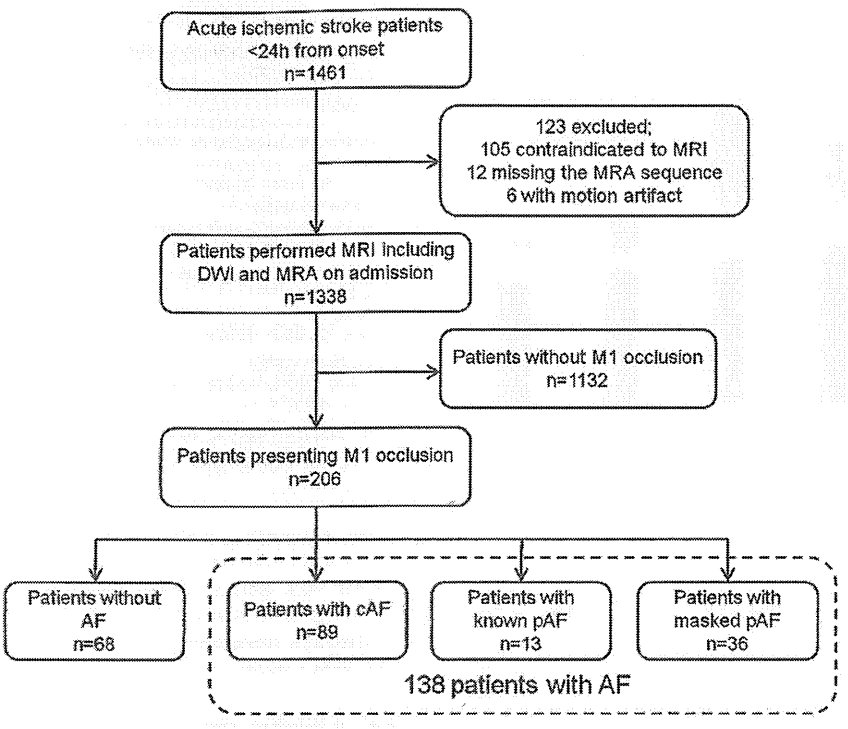

Fig. 1. Patient flow chart.

DWI-ASPECTS could distinguish patients with unidentified AF at presentation that was later documented from those with sinus rhythm.

The finding that DWI-ASPECTS discriminates patients with AF from those without AF was partly consistent with previous reports that showed a larger infarct volume on DWI in patients with cardioembolism than in those with internal carotid artery disease [4]. For acute stroke patients with M1 occlusion, AF seems to cause sudden main trunk occlusion and poor collateral circulation, and it may result in extensive ischemia [10]. However, visual assessment of the infarct volume depends on the reader's experience and skill and is time-consuming, and the intra-rater and inter-rater reliabilities are not sufficiently high [11]. On the other hand, DWI-ASPECTS can be scored promptly with good inter-rater reliability [5], and it is a simple and handy indicator in the emergent clinical setting. The cut-off of DWI-ASPECTS >6 was proven to be associated with complete or functional independency 3 months after IV t-PA [6,12]. The one-third of cerebral hemisphere rule on CT [13] appears to generally coincide with this cut-off of ASPECTS. In addition, AF was recently reported to predict poor outcome after IV t-PA [14,15]. The positive association of AF with DWI-ASPECTS ≤6 in our cohorts can be a good explanation for poor outcome of AF patients after thrombolysis.

The occluded sites of the M1 affect various clinical characteristics, including neurological severity, initial ASPECTS, and response to thrombolytic therapy [9]. It is interesting that DWI-ASPECTS ≤6 predicted

Table 1
Baseline characteristics.

Variables	Total	AF group	Non-AF group	p
	n=206	n=138	n=68	
Male sex, n (%)	111 (54)	67 (49)	44 (65)	0.037
Age, y, median (IQR)	77 (69–85)	80 (71–88)	74 (68–79)	<0.001
Vascular risk factors, n (%)				
Hypertension	144 (70)	95 (69)	49 (72)	0.747
Diabetes mellitus	28 (14)	14 (10)	14 (21)	0.051
Hyperlipidemia	69 (34)	37 (27)	32 (47)	0.005
Current smoking	41 (20)	18 (13)	23 (34)	0.001
Alcohol intake	77 (37%)	48 (35%)	29 (43%)	0.461
Blood pressure on admission, median (IQR)				
Systolic, mm Hg	156 (136–169)	153 (134–165)	160 (140–176)	0.115
Diastolic, mm Hg	83 (70–91)	82 (70–91)	84 (72–91)	0.777
Time from onset to initial MRI, h, median (IQR)	2.5 (1.5–8.2)	2.5 (1.5–7.9)	2.6 (1.5–8.7)	0.873
NIHSS score, median (IQR)	18 (13–23)	20 (15–23)	16 (12–20)	0.002
M1 proximal occlusion, n (%)	121 (59)	82 (59)	39 (57)	0.880
DWI-ASPECTS, median (IQR)	5 (3–7)	4 (2–6)	7 (4–8)	<0.001
Biochemistry results on admission, median (IQR)				
Leukocyte count, /μl	7300 (5700–9000)	7200 (5600–8900)	7900 (6200–9300)	0.120
hs-CRP, mg/dl	0.13 (0.06–0.53)	0.14 (0.06–0.59)	0.13 (0.06–0.45)	0.571
D-dimer, μg/ml	1.9 (1.2–3.5)	2.2 (1.3–4.0)	1.6 (1.0–2.6)	0.017

AF indicates atrial fibrillation; MRI, magnetic resonance imaging; NIHSS, National Institutes of Health stroke scale; M1, middle cerebral artery horizontal segment; hs-CRP, high-sensitivity C-reactive protein; DWI-ASPECTS, Alberta Stroke Program Early CT Score on diffusion-weighted imaging.

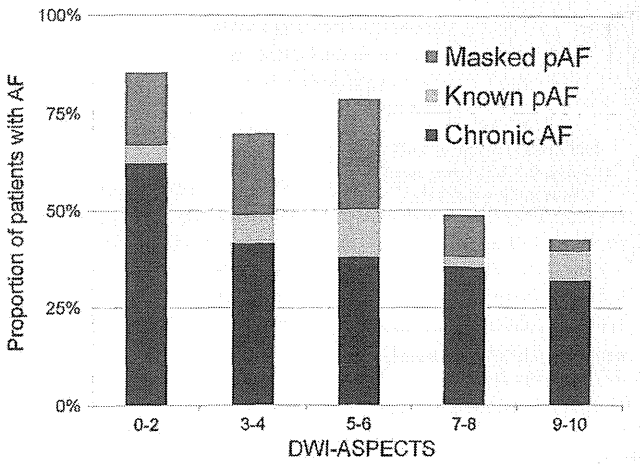

Fig. 2. The frequency of atrial fibrillation and the DWI-ASPECTS. The frequency of atrial fibrillation decreases along with the increase in DWI-ASPECTS ($r = -0.843$, $p = 0.001$ with Spearman's rank correlation test).

the presence of AF irrespective of the occluded sites. Atherosclerotic change in the MCA occurs predominantly in the stem [16], and embolic occlusion due to AF seems to be relatively common in the distal trunk where the caliber becomes smaller. Similar percentages of M1 proximal occlusion in the present AF and non-AF groups suggest that our cohort included many patients having large cardiogenic emboli.

Paroxysmal AF has similar risks of ischemic stroke to cAF [17,18] and is more prevalent than cAF in acute stroke patients [19]. Although guidelines recommend 24-h holter monitoring for patients with ischemic stroke of unknown cause [20], 24-h monitoring was reported to misdiagnose pAF in more than half of patients with confirmed pAF using 7-day Holter monitoring [1]. The left atrial volume index divided by diastolic velocity on echocardiogram and frequent atrial premature beats on ECG were other predictors of pAF in acute stroke [21,22], but their predictive values are not known. The present finding that DWI-ASPECTS predicted masked pAF even after removal of patients with cAF and previously known pAF helps in the quick selection of possible cardioembolic cases from cryptogenic stroke patients.

This study had some limitations. First, the retrospective design might have contributed to some selection bias. Second, ASPECTS is validated for ischemic strokes in the MCA territory, and the present finding cannot be applied to patients developing ischemic stroke in the posterior circulation. In addition, patients with MCA branch occlusion were not evaluated. Third, although every attempt was made to detect AF, some patients with pAF might have been overlooked. Fourth, most of the included patients were admitted and performed MRI in ultra-early phase in the present study. The median onset-to-MRI time was 2.5 h in this study, and our results should be carefully interpreted in generalization.

Table 2
Multivariate logistic regression analysis for predicting the presence of atrial fibrillation.

Variables	OR	95% CI	P
Male sex	0.65	0.30–1.41	0.276
Age (for every 10 years)	1.47	1.03–2.09	0.034
Diabetes mellitus	0.43	0.16–1.14	0.090
Hyperlipidemia	0.48	0.24–0.99	0.047
Current smoking	0.31	0.13–0.73	0.007
Initial NIHSS (for every 1 point)	1.01	0.96–1.07	0.635
DWI-ASPECTS ≤6	5.05	2.36–10.8	<0.001
D-dimer (for every 1.0 μg/ml)	1.04	0.91–1.19	0.587
DWI-ASPECTS (for every 1 point)	0.76	0.65–0.88	<0.001

NIHSS indicates the National Institutes of Health stroke scale; DWI-ASPECTS, Alberta Stroke Program Early CT Score on diffusion-weighted imaging.

Table 3
Multivariate logistic regression analyses for predicting the presence of paroxysmal atrial fibrillation (pAF).

Variables	OR	95% CI	p
Any pAF (both known and masked)			
Male sex	0.42	0.16–1.12	0.084
Age (for every 10 years)	1.66	1.00–2.75	0.050
Diabetes Mellitus	0.11	0.02–0.64	0.014
Initial NIHSS (for every 1 point)	1.04	0.96–1.13	0.306
DWI-ASPECTS ≤6	8.64	3.00–24.9	<0.001
D-dimer (for every 1.0 μg/ml)	0.98	0.84–1.15	0.820
Masked pAF			
Male sex	0.49	0.17–1.43	0.191
Age (for every 10 years)	1.80	1.05–3.06	0.031
Diabetes mellitus	0.16	0.03–0.90	0.038
Initial NIHSS (for every 1 point)	1.02	0.94–1.12	0.582
DWI-ASPECTS ≤6	10.0	3.06–32.9	<0.001

NIHSS indicates National Institutes of Health stroke scale; DWI-ASPECTS, Alberta Stroke Program Early CT Score on diffusion-weighted imaging.

In conclusion, extensive early ischemic change assessed by DWI-ASPECTS can discriminate the presence of AF from sinus rhythm in patients with acute ischemic stroke due to M1 occlusion, irrespective of the type of AF and the occluded site. DWI-ASPECTS ≤6 is a good indicator for thorough investigation of AF, including, for example, using implantable cardiac monitors.

Role of funding source

None.

Conflict of interest statement

M.K. receives grant support from the Japan Cardiovascular Research Foundation. K.T. and K.N. receive support from Grants-in-Aid, MHLW-Japan. K.M. receives support from Astellas Pharma Inc., Takeda Pharmaceutical Company Limited, Sanofi-Aventis, Lundbeck Inc., Mitsubishi-Tanabe Pharma Corporation, Kyowa-Hakko-Kirin Pharma Inc., Hitachi Medical Corporation, Research Grants for Cardiovascular Diseases and Grants-in-Aid from MHLW-Japan, and the Foundation for Biomedical Research and Innovation.

Acknowledgements

None.

References

[1] Stahrenberg R, Weber-Kruger M, Seegers J, Edelmann F, Lahno R, Haase B, et al. Enhanced detection of paroxysmal atrial fibrillation by early and prolonged continuous holter monitoring in patients with cerebral ischemia presenting in sinus rhythm. Stroke 2010;41:2884–8.
[2] Minematsu K, Li L, Fisher M, Sotak CH, Davis MA, Fiandaca MS. Diffusion-weighted magnetic resonance imaging: rapid and quantitative detection of focal brain ischemia. Neurology 1992;42:235–40.
[3] Lee LJ, Kidwell CS, Alger J, Starkman S, Saver JL. Impact on stroke subtype diagnosis of early diffusion-weighted magnetic resonance imaging and magnetic resonance angiography. Stroke 2000;31:1081–9.
[4] Jung JM, Kwon SU, Lee JH, Kang DW. Difference in infarct volume and patterns between cardioembolism and internal carotid artery disease: focus on the degree of cardioembolic risk and carotid stenosis. Cerebrovasc Dis 2010;29:490–6.
[5] Barber PA, Hill MD, Eliasziw M, Demchuk AM, Pexman JH, Hudon ME, et al. Imaging of the brain in acute ischaemic stroke: comparison of computed tomography and magnetic resonance diffusion-weighted imaging. J Neurol Neurosurg Psychiatry 2005;76:1528–33.
[6] Nezu T, Koga M, Kimura K, Shiokawa Y, Nakagawara J, Furui E, et al. Pretreatment ASPECTS on DWI predicts 3-month outcome following rt-PA: SAMURAI rt-PA Registry. Neurology 2010;75:555–61.
[7] Morita N, Harada M, Uno M, Matsubara S, Nagahiro S, Nishitani H. Evaluation of initial diffusion-weighted image findings in acute stroke patients using a semi-quantitative score. Magn Reson Med Sci 2009;8:47–53.
[8] Terasawa Y, Kimura K, Iguchi Y, Kobayashi K, Aoki J, Shibazaki K, et al. Could clinical diffusion-mismatch determined using DWI ASPECTS predict neurological

improvement after thrombolysis before 3 h after acute stroke? J Neurol Neurosurg Psychiatry 2010;81:864-8.
[9] Hirano T, Sasaki M, Mori E, Minematsu K, Nakagawara J, Yamaguchi T. Residual vessel length on magnetic resonance angiography identifies poor responders to alteplase in acute middle cerebral artery occlusion patients: exploratory analysis of the Japan Alteplase Clinical Trial II. Stroke 2010;41:2828-33.
[10] Kim SJ, Ryoo S, Kim GM, Chung CS, Lee KH, Bang OY. Clinical and radiological outcomes after intracranial atherosclerotic stroke: a comprehensive approach comparing stroke subtypes. Cerebrovasc Dis 2011;31:427-34.
[11] Rivers CS, Wardlaw JM, Armitage PA, Bastin ME, Hand PJ, Dennis MS. Acute ischemic stroke lesion measurement on diffusion-weighted imaging — important considerations in designing acute stroke trials with magnetic resonance imaging. J Stroke Cerebrovasc Dis 2007;16:64-70.
[12] Nakashima T, Toyoda K, Koga M, Matsuoka H, Nagatsuka K, Takada T, et al. Arterial occlusion sites on magnetic resonance angiography influence the efficacy of intravenous low-dose (0.6 mg/kg) alteplase therapy for ischaemic stroke. Int J Stroke 2009;4:425-31.
[13] von Kummer R, Allen KL, Holle R, Bozzao L, Bastianello S, Manelfe C, et al. Acute stroke: usefulness of early CT findings before thrombolytic therapy. Radiology 1997;205:327-33.
[14] Kimura K, Iguchi Y, Shibazaki K, Iwanaga T, Yamashita S, Aoki J. IV t-PA therapy in acute stroke patients with atrial fibrillation. J Neurol Sci 2009;276:6-8.
[15] Seet RC, Zhang Y, Wijdicks EF, Rabinstein AA. Relationship between chronic atrial fibrillation and worse outcomes in stroke patients after intravenous thrombolysis. Arch Neurol 2011;68:1454-8.
[16] Mohr JP, Lazar RM, Marshall RS. Middle cerebral artery disease. In: Mohr JP, Wolf PA, Grotta JC, Moskowitz MA, Mayberg MR, Kummer R, editors. Stroke: pathophysiology, diagnosis, and management. 5th ed. Elsevier; 2011. p. 384-424.
[17] Hohnloser SH, Pajitnev D, Pogue J, Healey JS, Pfeffer MA, Yusuf S, et al. Incidence of stroke in paroxysmal versus sustained atrial fibrillation in patients taking oral anticoagulation or combined antiplatelet therapy: an ACTIVE W Substudy. J Am Coll Cardiol 2007;50:2156-61.
[18] Stollberger C, Chnupa P, Abzieher C, Langer T, Finsterer J, Klem I, et al. Mortality and rate of stroke or embolism in atrial fibrillation during long-term follow-up in the embolism in left atrial thrombi (ELAT) study. Clin Cardiol 2004;27:40-6.
[19] Rizos T, Wagner A, Jenetzky E, Ringleb PA, Becker R, Hacke W, et al. Paroxysmal atrial fibrillation is more prevalent than persistent atrial fibrillation in acute stroke and transient ischemic attack patients. Cerebrovasc Dis 2011;32:276-82.
[20] European Stroke Organisation Executive Committee. Guidelines for management of ischaemic stroke and transient ischaemic attack 2008. Cerebrovasc Dis 2008;25:457-507.
[21] Stahrenberg R, Edelmann F, Haase B, Lahno R, Seegers J, Weber-Kruger M, et al. Transthoracic echocardiography to rule out paroxysmal atrial fibrillation as a cause of stroke or transient ischemic attack. Stroke 2011;42:3643-5.
[22] Wallmann D, Tuller D, Wustmann K, Meier P, Isenegger J, Arnold M, et al. Frequent atrial premature beats predict paroxysmal atrial fibrillation in stroke patients: an opportunity for a new diagnostic strategy. Stroke 2007;38:2292-4.

Original Paper

Cerebrovascular Diseases

Cerebrovasc Dis 2012;33:272–279
DOI: 10.1159/000333449

Received: September 20, 2010
Accepted: September 16, 2011
Published online: January 26, 2012

Visibility of the Lesser Sphenoid Wing Is an Important Indicator for Detecting the Middle Cerebral Artery on Transcranial Color-Coded Sonography

Rieko Suzuki[a] Masatoshi Koga[b] Mayumi Mori[a] Kaoru Endo[a]
Kazunori Toyoda[a] Kazuo Minematsu[a]

[a]Department of Cerebrovascular Medicine and [b]Division of Stroke Care Unit, National Cerebral and Cardiovascular Center, Osaka, Japan

Key Words
Cerebrovascular disease · Lesser sphenoid wing · Middle cerebral artery · Transcranial color-coded sonography · Stroke

Abstract
Background: Failure to detect the sphenoidal segment of the middle cerebral artery (M1) on transcranial color-coded sonography (TCCS) results from either M1 occlusion or an insufficient temporal bone window (TBW). We sought to identify a simple indicator on B mode images for M1 evaluation. ***Methods:*** Consecutive acute ischemic stroke patients with an intact M1 segment underwent prospective TCCS evaluation. Visibilities of the contralateral temporal bone (CTB), midbrain (MB) and lesser sphenoid wing (LSW) on B mode images were defined as follows: 'invisible', 'poor' if the contour was less than 50% visible, 'fair' if more than 50% visible and 'good' if totally visible. M1 detectability on color Doppler images was defined as follows: 'INVISIBLE', 'POOR' if the M1 was detected as color dots, 'FAIR' if linearly but discontinuously detectable, and 'GOOD' if linearly and continuously detectable. The relationship between each structure's visibility and M1 detectability was assessed. ***Results:*** Seventy-six patients with 152 TBWs were evaluated. The CTB was 'invisible' in 2%, 'poor' in 22%, 'fair' in 36% and 'good' in 40%. Visibility of the MB was 36, 24, 26 and 14%, respectively. Visibility of the LSW was 16, 22, 29 and 32%, respectively. The M1 was 'INVISIBLE' in 51%, 'POOR' in 7%, 'FAIR' in 7% and 'GOOD' in 35%. Spearman's rank correlation coefficient between each structure's visibility and M1 detectability was 0.68 for the CTB, 0.66 for the MB and 0.80 for the LSW, respectively ($p < 0.001$ for all). ***Conclusion:*** Visibility of the LSW on B mode appears to be a better indicator than other structures for M1 evaluation.

Background

Transcranial color-coded duplex sonography (TCCS) is widely used to evaluate the intracranial arterial system in patients with acute stroke [1–4]. There have been insufficient data to compare the ability of ultrasonographic examination to visualize intracranial structures and vessels through the skull bone in different races [5–7]. There is some reported data on success rates for Doppler ultrasound in different races, with the highest success rates in northern Europeans, and lower in most other populations (Asians, African Americans, Hispanics) [8–10].

KARGER

Fax +41 61 306 12 34
E-Mail karger@karger.ch
www.karger.com

1015–9770/12/0333–0272$38.00/0

Accessible online at:
www.karger.com/ced

Masatoshi Koga, MD
Division of Stroke Care Unit
National Cerebral and Cardiovascular Center
Osaka 565-8565 (Japan)
Tel. +81 6 6833 5012, E-Mail koga@hsp.ncvc.go.jp

There is much less reported data on relative success rates in different races for intracranial B mode imaging. Asian populations have a high frequency of poor temporal bone windows (TBWs) [8–10]; failure to detect the sphenoidal portion of the middle cerebral artery (M1) on TCCS could be secondary to M1 occlusion or to an inadequate TBW, or sometimes to poor technique or wrong gain settings. The hyperechoic lesser sphenoid wing and superior margin of the petrous pyramid were proposed to be indicators for the identification of the middle and posterior cerebral arteries [11]. This study aimed to clarify the relationship between visibilities of the contralateral temporal bone (CTB), midbrain (MB) and ipsilateral lesser sphenoid wing (LSW) on B mode images and the detectability of the ipsilateral M1 on color Doppler images by TCCS. We have attempted to develop a simple indicator to determine whether failure to detect flow in the M1 is secondary to local arterial disease or to an inadequate bone window.

Subjects and Methods

Consecutive patients with acute ischemic stroke admitted to our stroke center within 7 days after stroke onset between January 2009 and July 2009 were prospectively registered. They were evaluated by intracranial magnetic resonance imaging (MRI) for brain and intracranial magnetic resonance angiography (MRA) for intracranial arteries with a 1.5-tesla system (Magnetom Vision; Siemens, Germany), and carotid duplex ultrasonography for the common carotid artery and the extracranial internal carotid artery (ICA) using a Hitachi EUB-8500 ultrasound machine (Hitachi Medical Corp, Tokyo, Japan) with a 7.5-MHz linear probe on admission. Patients having an M1 or an ICA with luminal stenosis >50% or occlusion on baseline intracranial MRA or carotid ultrasonography, those having a pacemaker, or those who had an extracranial-intracranial arterial bypass were excluded from our study.

TCCS Examination

TCCS examination using a Hitachi EUB-8500 ultrasound machine with a 2- to 2.5-MHz sector probe was performed transtemporally in horizontal projection within 24 h after initial MRA and carotid US evaluations. Patients were lying in a supine, left lateral or right lateral decubitus position according to the side of the TBW examined and the patient's condition. With a scanning depth of 15.5 cm as a fixed depth, the CTB was visualized first for orientation, and the visibilities of the CTB, MB and LSW were assessed. On B mode images, the MB is hypoechoic and butterfly-shaped, and it is surrounded by hyperechoic subarachnoid cisterns, and the LSW has a hyperechoic outline of the bony structures at the skull base [11]. The B mode gain was initially set at 20 and adjusted to optimize structure delineation in the ultrasound image. Then color Doppler ultrasound was used to identify the intracranial arteries. The color gain was set at 38 as a default value and adjusted to obtain an optimum color display to the setting just below that in which background noise first becomes apparent. The velocity color scale was initially set at ±27.3 cm/s. To mitigate aliasing, color flow velocity settings were changed between ±2.3 and ±54.7 cm/s. The M1 at a depth of 4–6 cm was evaluated as a unidirectional flow toward the probe on color Doppler images. If color dots or discontinuous color were initially detected, whether the vessel was the M1 or not was judged based on the depth, the positional relationships with the probe and the intracranial structures, and the direction of blood flow, and further attempts to manipulate the probe superiorly and inferiorly to identify the remainder of the M1 were performed. If the MB and LSW could not be clearly identified, we carefully measured the intracranial head diameter by using the B mode and used the actual depth to guide the examination. Two experienced vascular neurologists who knew the information of the M1 on baseline MRA assessed the visibilities of the MB, LSW and CTB on B mode images and assigned patients into 4 categories as follows: 'invisible' if the hyperechoic CTB within the echo window, the peduncle of the MB or the hyperechoic LSW within the echo window was not visible at all; 'poor' if it was visible less than 50%; 'fair' if it was visible more than 50%, and 'good' if it was almost totally visible (fig. 1, 2). The detectability of the M1 was assessed on color Doppler images and assigned into similar categories as follows: 'INVISIBLE' if the M1 was undetected, 'POOR' if detected as color dots, 'FAIR' if linearly but discontinuously detectable and 'GOOD' for being linearly and continuously detectable (fig. 2, 3). When the M1 was assigned into the category 'INVISIBLE', the detectabilities of the anterior and posterior cerebral arteries from the same TBW were also evaluated to ascertain the absence of a proper TBW according to the recent consensus recommendations [4]. The posterior cerebral artery was detectable if the precommunicating segment, proximal or distal postcommunicating segment was detected. The interrater and intrarater agreements for each of the categories (invisible, poor, fair and good), by kappa statistic, were 0.45 and 0.64 for the MB, 0.62 and 0.85 for the LSW, 0.61 and 0.71 for the CTB, and 0.89 and 0.96 for the M1, respectively, according to the offline video monitoring evaluations of 20 randomly selected patients by the above-mentioned two experienced vascular neurologists.

Contrast-Enhanced TCCS Examination

Contrast-enhanced TCCS examination was performed in the initial 10 patients who had 'INVISIBLE', 'POOR' or 'FAIR' detection of the M1 on color Doppler images after they had given their informed consent. Levovist (Bayer Health Care, Leverkusen, Germany), an ultrasound contrast agent consisting of granules composed of 99.9% galactose and 0.1% palmitic acid, was used. Levovist was injected at a dose of 2.5 g diluted in 7 ml of 0.9% saline resulting in a concentration of 300 mg/ml (total volume, 8.5 ml). A 4.25-ml bolus of Levovist was injected into an antecubital vein within 10 s, followed by a 10-ml saline chaser bolus for the one side. A second injection for the other side was administered after the first contrast effect had faded out. Detectability improvement on contrast-enhanced TCCS examination was defined as improvement of M1 detectability on contrast-enhanced TCCS by one or more categories compared with that on non-contrast-enhanced examination.

Data Analysis

The percentages of each finding were calculated for all patients, by sex and by age (<70 years old or ≥70 years old). The percent-

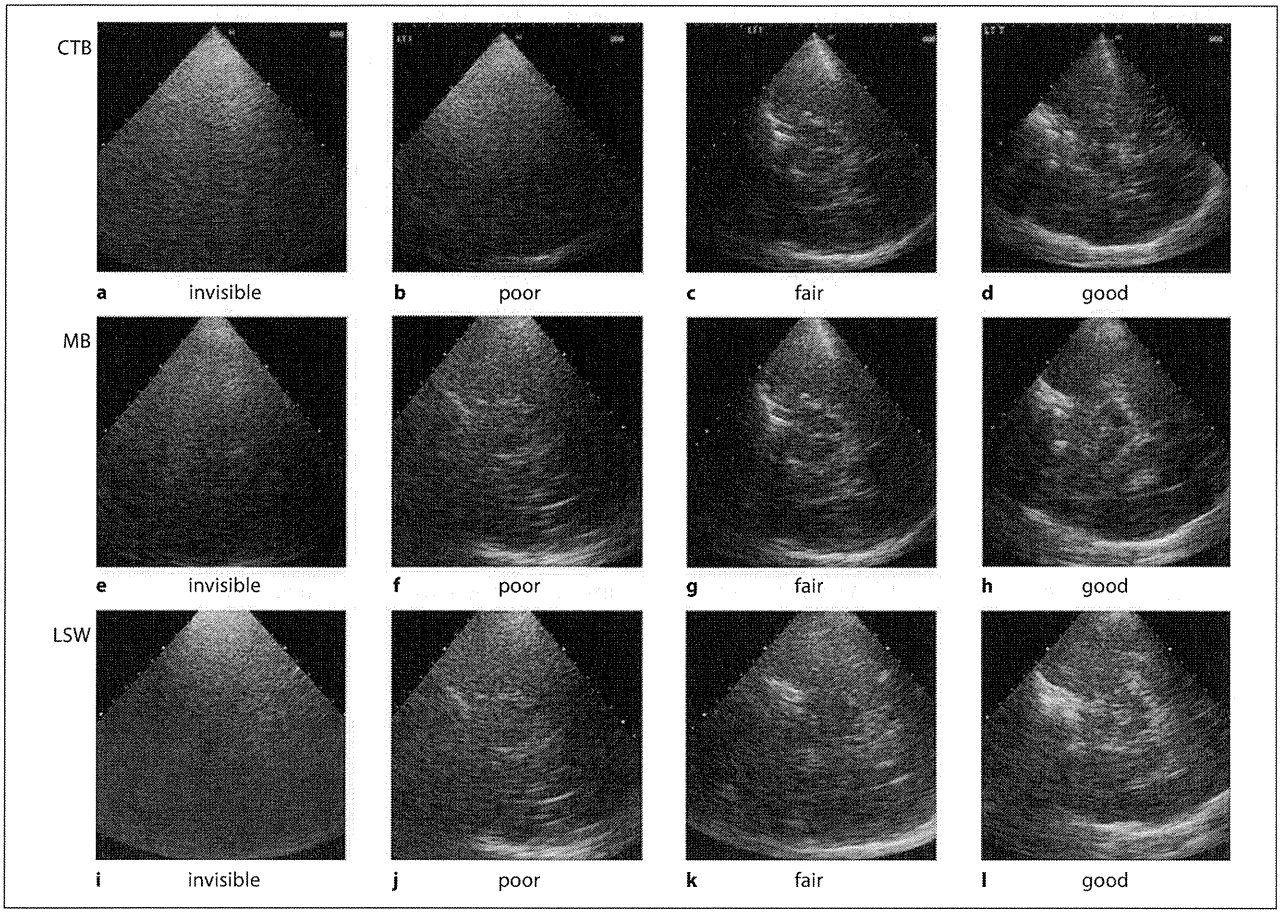

Fig. 1. Visibilities of CTB (**a–d**), MB (**e–h**) and LSW (**i–l**) on B mode images. invisible = The contour is not visible; poor = the contour is less than 50% visible; fair = the contour is more than 50% visible; good = the contour is almost totally visible.

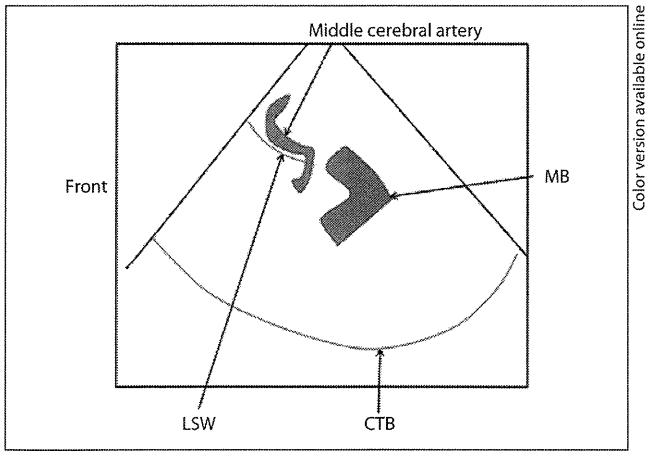

Fig. 2. A schema of CTB, MB, LSW and middle cerebral artery.

Color version available online

ages of each category were compared by sex and by age using the χ^2 test. The relationship between each structure's visibility and M1 detectability was analyzed using Spearman's rank correlation. The percentages of M1 detection improvement by categorical visibility of each structure on B mode images were calculated.

Results

One hundred and twenty-four acute ischemic stroke patients admitted to our stroke center during the study period were investigated. Forty-six patients who had vascular abnormality on MRA (13 ICA occlusion, 5 ICA stenosis ≥50%, 1 ICA pseudo-occlusion, 14 middle cerebral artery M1 occlusion, 13 middle cerebral artery M1 stenosis ≥50%), 1 patient having a pacemaker, and 1 patient

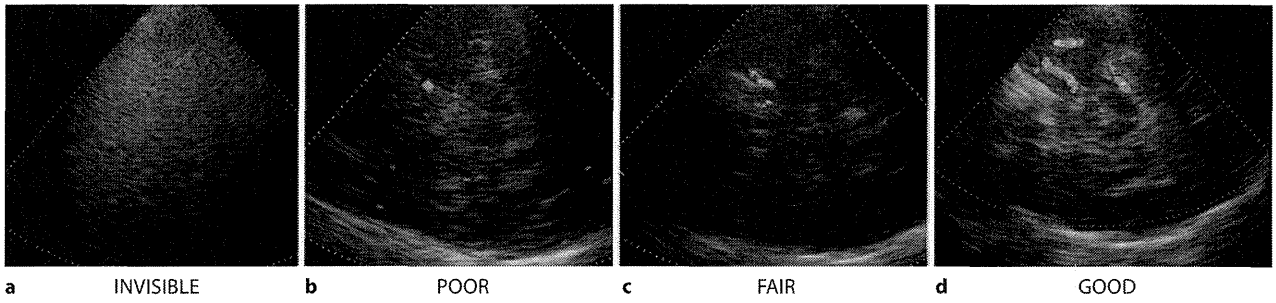

Fig. 3. M1 detectability on color Doppler images. **a** The M1 is undetectable (INVISIBLE). **b** The M1 is detected as color dots (POOR). **c** The M1 is linearly but discontinuously detectable (FAIR). **d** The M1 is linearly and continuously detectable (GOOD).

who had superficial temporal artery/middle cerebral artery anastomosis were excluded. Seventy-six patients (48 men, 71 ± 12 years old) with 152 TBWs were evaluated by TCCS. None of these had a large infarction which caused brain displacement on MRI. Table 1 summarizes the percentages of each structure's visibility on B mode images and M1 detectability on color Doppler images for all patients, by sex and by age. There were 38 TBWs of women aged ≥70 years, 42 TBWs of men aged ≥70 years, 18 TBWs of women aged <70 years and 54 TBWs of men <70 years. The CTB, MB and LSW were visible on B mode in 98, 64 and 84%, respectively; levels of visibility are shown in table 1. The M1 was detected in 49% on color Doppler images, and M1 detectability was 'POOR' in 7%, 'FAIR' in 7% and 'GOOD' in 35%. Structural visibilities on B mode and M1 detectability were better in men than in women and in younger adults (<70 years old) than in older adults (≥70 years old). Among 77 TBWs with an 'INVISIBLE' M1, the anterior cerebral artery was detectable only through 4 TBWs, and the PCA was detectable through 25 TBWs (table 2).

The correlation coefficient between each structure's visibility and M1 detectability was 0.68 for the CTB, 0.66 for the MB and 0.80 for the LSW ($p < 0.001$ for all; table 3). The M1 was detectable as 'GOOD' in 40 (82%) out of 49 TBWs with 'good' LSW visibility, although it was so in 43 (70%) out of 61 TBWs with 'good' CTB visibility and in 17 (77%) out of 22 TBWs with 'good' MB visibility. When the LSW was invisible, the M1 was not detected. When the LSW was less than 50% visible, the M1 was detected in 9%. When the LSW was more than 50% visible, the M1 was detected in 55%. When the LSW was almost totally visible, the M1 was detected in 98%. The correlation coefficients between each structure's visibility and M1 detectability in men were 0.62 for the CTB, 0.60 for the MB and 0.74 for the LSW ($p < 0.001$ for all); those in women were 0.58, 0.53 and 0.72, respectively ($p < 0.001$ for all). Those of younger adults were 0.61, 0.58 and 0.74, respectively ($p < 0.001$ for all); those of older adults were 0.71, 0.70 and 0.80, respectively ($p < 0.001$ for all).

Contrast-enhanced TCCS examination was performed in 20 TBWs of 10 patients (table 4). In 8 of 20 TBWs (40%), the M1 was identified with 1 or more category improvements compared with that on non-contrast-enhanced examination. The detection improvement of the M1 was ascertained for no TBWs with 'invisible' LSW, 50% with 'poor' LSW, 57% with 'fair' LSW and 50% with 'good' LSW.

Discussion

In this study, categorical visibilities of the CTB, MB and LSW on B mode images and categorical M1 detectability on color Doppler images by TCCS were determined in Japanese acute ischemic stroke patients without stenotic lesions of the M1 or ICA on baseline MRA or carotid ultrasonography. The major findings were as follows: first, the M1 was detectable by TCCS in 49% in this study of patients with a known patent M1. Second, visibilities of the CTB, MB and LSW on B mode images had positive correlations with M1 detectability on color Doppler images. Third, LSW visibility was a better indicator than CTB and MB visibilities for evaluation of the M1. Fourth, contrast-enhanced TCCS examination provided better M1 detection than nonenhanced examination in half of the TBWs through which each structure was vis-

Table 1. Structural visualization and M1 detectability by TCCS

Structural visualization on B mode image		invisible	visible			p
			poor	fair	good	
Structural visualization on B mode image						
CTB	Total (152 TBWs)	3 (2)	34 (22)	54 (36)	61 (40)	
	Women (56 TBWs)	3 (5)	25 (45)	16 (29)	12 (21)	<0.0001[a]
	Men (96 TBWs)	0	9 (9)	38 (40)	39 (51)	
	Aged ≥70 years (80 TBWs)	3 (4)	23 (29)	30 (38)	24 (30)	0.0163[b]
	Aged <70 years (72 TBWs)	0	11 (15)	24 (33)	37 (51)	
	Women aged ≥70 years (38 TBWs)	3 (8)	20 (53)	10 (26)	5 (13)	0.0689[c]
	Women aged <70 years (18 TBWs)	0	5 (28)	6 (33)	7 (39)	
	Men aged ≥70 years (42 TBWs)	0	3 (7)	20 (48)	19 (45)	0.3486[d]
	Men aged <70 years (54 TBWs)	0	6 (11)	18 (33)	30 (56)	
MB	Total (152 TBWs)	55 (36)	36 (24)	39 (26)	22 (14)	
	Women (56 TBWs)	37 (66)	10 (18)	7 (13)	2 (4)	<0.0001[a]
	Men (96 TBWs)	18 (19)	26 (27)	32 (33)	20 (21)	
	Aged ≥70 years (80 TBWs)	39 (49)	22 (28)	17 (21)	2 (3)	<0.0001[b]
	Aged <70 years (72 TBWs)	16 (22)	14 (19)	22 (31)	20 (28)	
	Women aged ≥70 years (38 TBWs)	30 (79)	6 (16)	2 (5)	0	0.0061[c]
	Women aged <70 years (18 TBWs)	7 (39)	4 (22)	5 (28)	2 (11)	
	Men aged ≥70 years (42 TBWs)	9 (21)	16 (38)	15 (36)	2 (5)	0.0046[d]
	Men aged <70 years (54 TBWs)	9 (17)	10 (19)	17 (31)	18 (33)	
LSW	Total (152 TBWs)	25 (16)	34 (22)	44 (29)	49 (32)	
	Women (56 TBWs)	15 (27)	23 (41)	10 (18)	8 (14)	<0.0001[a]
	Men (96 TBWs)	10 (10)	11 (11)	34 (35)	41 (43)	
	Aged ≥70 years (80 TBWs)	16 (20)	22 (28)	23 (29)	19 (24)	0.0700[b]
	Aged <70 years (72 TBWs)	9 (13)	12 (17)	21 (29)	30 (42)	
	Women aged ≥70 years (38 TBWs)	13 (34)	16 (42)	5 (13)	4 (11)	0.1649[c]
	Women aged <70 years (18 TBWs)	2 (11)	7 (39)	5 (28)	4 (22)	
	Men aged ≥70 years (42 TBWs)	3 (7)	6 (14)	18 (43)	15 (36)	0.3460[d]
	Men aged <70 years (54 TBWs)	7 (13)	5 (9)	16 (30)	26 (48)	
M1 detectability on color Doppler images		INVISIBLE	POOR	FAIR	GOOD	p
M1	Total (152 TBWs)	77 (51)	11 (7)	11 (7)	53 (35)	
	Women (56 TBWs)	42 (75)	3 (5)	2 (4)	9 (16)	<0.0001[a]
	Men (96 TBWs)	35 (36)	8 (8)	9 (9)	44 (46)	
	Aged ≥70 years (80 TBWs)	46 (58)	8 (10)	7 (9)	19 (24)	0.0198[b]
	Aged <70 years (72 TBWs)	31 (43)	3 (4)	4 (6)	34 (47)	
	Women aged ≥70 years (38 TBWs)	29 (76)	3 (8)	1 (3)	5 (13)	0.5002[c]
	Women aged <70 years (18 TBWs)	13 (72)	0	1 (6)	4 (22)	
	Men aged ≥70 years (42 TBWs)	17 (40)	5 (12)	6 (14)	14 (33)	0.1146[d]
	Men aged <70 years (54 TBWs)	18 (33)	3 (6)	3 (6)	30 (56)	

Values are represented by numbers of TBWs, with percentages in parentheses.
[a] Women versus men by χ^2 test. [b] Aged ≥70 years versus aged <70 years by χ^2 test. [c] Women aged ≥70 years versus women aged <70 years by χ^2 test. [d] Men aged ≥70 years versus men aged <70 years by χ^2 test.

ible ('poor', 'fair' or 'good'), whereas TBWs with 'invisible' MB or LSW could not gain any contrast improvement for M1 detection.

TCCS is widely used to evaluate the intracranial arterial system in patients with acute stroke. The main limitation of TCCS arises from poor acoustic insonation conditions via the TBW, particularly in Asians, women and older patients. The failure rate because of an insufficient acoustic bone window is approximately 10–20% of patients in Western countries [8–10] and 20–30% of

Table 2. Anterior (ACA) and posterior cerebral artery (segment 1 and 2) detectabilities of 77 TBWs with 'INVISIBLE' M1

	INVISIBLE	POOR	FAIR	GOOD
ACA	73	3	1	0
P1	71	5	1	0
Proximal P2	59	10	6	2
Distal P2	57	4	11	5

Values are represented by numbers of TBWs.

Table 3. Relationship between structural visualization and M1 detectability

		M1 detectability				Spearman's ρ	p
		INVISIBLE	POOR	FAIR	GOOD		
CTB	invisible (3 TBWs)	3	0	0	0	0.68	<0.0001
	poor (34 TBWs)	33	0	1	0		
	fair (54 TBWs)	32	8	4	10		
	good (61 TBWs)	9	3	6	43		
MB	invisible (55 TBWs)	48	5	1	1	0.66	<0.0001
	poor (36 TBWs)	19	3	4	10		
	fair (39 TBWs)	7	2	5	25		
	good (22 TBWs)	3	1	1	17		
LSW	invisible (25 TBWs)	25	0	0	0	0.80	<0.0001
	poor (34 TBWs)	31	2	1	0		
	fair (44 TBWs)	20	6	5	13		
	good (49 TBWs)	1	3	5	40		

Values are represented by numbers of TBWs.

patients in Asian countries [4, 5]. In our study, this rate was 51%. Low M1 detectability in women and older patients was consistent with previous reports [9, 10]. Therefore, simple indicators to judge acoustic insonation conditions via the TBW are important to evaluate the M1 segment.

Insonations of B mode and color Doppler seem to be similarly affected by the temporal bone, because structural visibilities on B-mode images had significantly positive correlations with M1 detectability on color Doppler images for all patients, by sex and by age. The closer spatial relationship of the M1 with the LSW than with the CTB or MB seems to explain the present results that LSW visibility had the best correlation with M1 detectability. When the M1 was 'INVISIBLE' on color Doppler images, the precommunicating segment, proximal and distal postcommunicating segments were detected in 32% but the anterior cerebral artery was rarely detectable via the same TBW. Based on our results, the following criteria for

Table 4. M1 detectability improvement by contrast enhancement

		Improvement of M1 detectability
CTB	invisible (0 TBWs)	–
	poor (4 TBWs)	0
	fair (5 TBWs)	1 (20)
	good (11 TBWs)	7 (64)
MB	invisible (6 TBWs)	0
	poor (7 TBWs)	4 (57)
	fair (4 TBWs)	3 (75)
	good (3 TBWs)	1 (33)
LSW	invisible (5 TBWs)	0
	poor (6 TBWs)	3 (50)
	fair (7 TBWs)	4 (57)
	good (2 TBWs)	1 (50)

Values are represented by numbers of TBWs, with percentages in parentheses.

M1 evaluation on TCCS were developed. If the LSW is almost totally visible, M1 occlusion may be considered in patients with M1 invisibility. If the LSW is invisible or less than 50% visible, M1 invisibility on TCCS does not directly indicate M1 occlusion, and an additional imaging modality, such as MRA or CT angiography, is required. If the LSW is more than 50% visible and the M1 is not detectable, more than 50% or totally, visibility of the CTB and MB indicates probable M1 occlusion.

The addition of an ultrasound contrast agent allows adequate diagnosis in about 80–90% of patients with insufficient bone windows [12–20]. In our Japanese stroke patients, 40% of TBWs had an improved detection of the M1 on contrast-enhanced examination. In patients with invisible structures on B mode images, the administration of a contrast agent did not result in vessel identification. Therefore, TBWs with poor, fair and good visibility and insufficient M1 detection seem to be appropriate candidates for contrast-enhanced TCCS examination.

There were some limitations in this study. First, M1 occlusion on TCCS cannot be discussed from our findings because of the study exclusion of patients with luminal stenosis >50% or occlusion of the M1 or ICA on MRA and those with large infarction which may cause brain displacement. Second, severe atherosclerosis often causes arterial tortuosity and calcification. Arterial tortuosity might shift the M1 further from the LSW, and calcification might prevent ultrasound insonation. Third, machine specificity might affect structural visibility and M1 detectability. Fourth, the small sample size might affect the statistical correlation between the M1 detectability and the visibility of each anatomical structure, and a larger study might be needed to confirm our results. Finally, because our vascular neurologists knew that all the patients had a patent M1, the results might be overestimated.

Conclusion

The visibility of the LSW on B mode images was well correlated with M1 detection in Japanese aged patients with acute ischemic stroke having a patent M1. Our findings warrant future studies to determine detailed criteria of M1 occlusion using TCCS in patients with acute ischemic stroke.

Acknowledgments

This study was supported in part by a Grant-in-Aid (H21-Trans-Ippan-008) from the Ministry of Health, Labor and Welfare of Japan, and a grant from the Japan Cardiovascular Research Foundation (the Bayer Scholarship for Cardiovascular Research).

Disclosure Statement

None.

References

1 Hou WH, Liu X, Duan YY, Wang J, Sun SG, Deng JP, Qin HZ, Cao TS: Evaluation of transcranial color-coded duplex sonography for cerebral artery stenosis or occlusion. Cerebrovasc Dis 2009;27:479–484.

2 Malferrari G, Bertolino C, Casoni F, Zini A, Sarra VM, Sanguigni S, Pratesi M, Lochner P, Coppo L, Brusa G, Guidetti D, Cavuto S, Marcello N: The eligible study: ultrasound assessment in acute ischemic stroke within 3 hours. Cerebrovasc Dis 2007;24:469–476.

3 Baumgartner RW: Transcranial color duplex sonography in cerebrovascular disease: a systematic review. Cerebrovasc Dis 2003;16:4–13.

4 Nedelmann M, Stolz E, Gerriets T, Baumgartner RW, Malferrari G, Seidel G, Kaps M: Consensus recommendations for transcranial color-coded duplex sonography for the assessment of intracranial arteries in clinical trials on acute stroke. Stroke 2009;40:3238–3244.

5 Seidel G, Kaps M, Gerriets T: Potential and limitations of transcranial color-coded sonography in stroke patients. Stroke 1995;26:2061–2066.

6 Kenton AR, Martin PJ, Abbott RJ, Moody AR: Comparison of transcranial color-coded sonography and magnetic resonance angiography in acute stroke. Stroke 1997;28:1601–1606.

7 Krejza J, Swiat M, Pawlak MA, Oszkinis G, Weigele J, Hurst RW, Kasner S: Suitability of temporal bone acoustic window: Conventional TCD versus transcranial color-coded duplex sonography. J Neuroimaging 2007;17:311–314.

8 Halsey JH: Effect of emitted power on waveform intensity in transcranial Doppler. Stroke 1990;21:1573–1578.

9 Itoh T, Matsumoto M, Handa N, Maeda H, Hougaku H, Hashimoto H, Etani H, Tsukamoto Y, Kamada T: Rate of successful recording of blood flow signals in the middle cerebral artery using transcranial Doppler sonography. Stroke 1993;24:1192–1195.

10 Yagita Y, Etani H, Handa N, Itoh T, Imuta N, Okamoto M, Matsumoto M, Kinoshita N, Nukada T: Effect of transcranial Doppler intensity on successful recording in Japanese patients. Ultrasound Med Biol 1996;22:701–705.

11 Krejza J, Mariak Z, Melhem ER, Bert RJ: A guide to the identification of major cerebral arteries with transcranial color Doppler sonography. AJR 2000;174:1297–1303.

12 Zunker P, Wilms H, Brossmann J, Georgiadis D, Weber S, Deuschl G: Echo contrast-enhanced transcranial ultrasound: frequency of use, diagnostic benefit, and validity of results compared with MRA. Stroke 2002;33:2600–2603.

13 Postert T, Braun B, Meves S, Koster O, Przuntek H, Weber S, Buttner T: Contrast-enhanced transcranial color-coded sonography in acute hemispheric brain infarction. Stroke 1999;30:1819–1826.
14 Gerriets T, Seidel G, Fiss I, Modrau B, Kaps M: Contrast-enhanced transcranial color-coded duplex sonography: efficiency and validity. Neurology 1999;52:1133–1137.
15 Baumgartner RW, Arnold M, Gonner F, Staikow I, Herrmann C, Rivoir A, Muri RM: Contrast-enhanced transcranial color-coded duplex sonography in ischemic cerebrovascular disease. Stroke 1997;28:2473–2478.
16 Bogdahn U, Becker G, Schlief R, Reddig J, Hassel W: Contrast-enhanced transcranial color-coded real-time sonography. Results of a phase-two study. Stroke 1993;24:676–684.
17 Goertler M, Kross R, Baeumer M, Jost S, Grote R, Weber S, Wallesch CW: Diagnostic impact and prognostic relevance of early contrast-enhanced transcranial color-coded duplex sonography in acute stroke. Stroke 1998;29:955–962.
18 Nabavi DG, Droste DW, Kemeny V, Schulte-Altedorneburg G, Weber S, Ringelstein EB: Potential and limitations of echocontrast-enhanced ultrasonography in acute stroke patients: a pilot study. Stroke 1998;29:949–954.
19 Kunz A, Hahn G, Mucha D, Muller A, Barrett KM, von Kummer R, Gahn G: Echo-enhanced transcranial color-coded duplex sonography in the diagnosis of cerebrovascular events: a validation study. AJNR Am J Neuroradiol 2006;27:2122–2127.
20 Seidel G, Meairs S: Ultrasound contrast agents in ischemic stroke. Cerebrovasc Dis 2009;27(suppl 2):25–39.

Original Paper

Cerebrovascular Diseases

Cerebrovasc Dis 2012;33:369–377
DOI: 10.1159/000336121

Received: March 22, 2011
Accepted: December 21, 2011
Published online: March 14, 2012

Identification of Internal Carotid Artery Dissection by Transoral Carotid Ultrasonography

Rieko Suzuki[a] Masatoshi Koga[b] Kazunori Toyoda[a] Masahiro Uemura[c]
Hikaru Nagasawa[a] Yusuke Yakushiji[a] Hiroshi Moriwaki[c] Naoaki Yamada[d]
Kazuo Minematsu[a]

[a]Department of Cerebrovascular Medicine, [b]Division of Stroke Care, [c]Department of Neurology, and
[d]Department of Radiology, National Cerebral and Cardiovascular Center, Suita, Japan

Key Words
Transoral carotid ultrasonography · Cerebrovascular disease · Internal carotid artery dissection · Stroke

Abstract
Background and Purpose: Conventional transsurface carotid ultrasonography (TSCU) via the cervical surface often fails to detect dissection of the extracranial internal carotid artery (ICA). The role of transoral carotid ultrasonography (TOCU) in the detection of ICA dissection was examined. ***Method:*** Patients with unilateral extracranial ICA dissection identified by digital subtraction angiography (DSA) from our database of patients with ischemic stroke or transient ischemic attack (TIA) were reviewed. Findings of dissection were compared between TSCU and TOCU. ***Results:*** Eight patients (7 men, 37–69 years old), including 7 with ischemic stroke and 1 with TIA, had ICA dissection. By DSA, dissection was identified between the first and third vertebrae in 4 patients and from the third cervical vertebra to the intracranial level in the remaining 4. TOCU images revealed an intimal flap as definite evidence of dissection in all patients. In 7 patients, color flow signals were not seen in false lumens, indicating thrombosed lumens. Four patients showed morphological changes of dissection on follow-up TOCU, including a patient with recovery of color flow signals in false lumens. The diameter of the dissected ICA was 7.3 ± 0.7 mm and that of the contralateral ICA was 4.9 ± 0.6 mm ($p = 0.008$). In contrast, TSCU did not enable any conclusive findings of ICA dissection to be made in any patient. Six patients had intramural hematoma on T_1-weighted MRI, and 2 had an intimal flap with a double lumen on magnetic resonance angiography. ***Conclusion:*** TOCU has advantages over TSCU in achieving an accurate diagnosis and follow-up evaluation of ICA dissection.

Introduction

Internal carotid arterial (ICA) dissection accounts for approximately 2–3% of all ischemic strokes [1, 2] and is one of the important causes of stroke in young and middle-aged patients [3–6]. The pathogenesis of ICA dissection is often unknown. Most ICA dissections occur spontaneously or follow a sudden head movement, a chiropractic manipulation, and many types of sports activities [7, 8]. Because ICA dissection sometimes causes brain ischemia and subarachnoid hemorrhage [6], immediate vascular evaluation and treatment are necessary. Among the diagnostic tools for identifying dissections, including

KARGER
Fax +41 61 306 12 34
E-Mail karger@karger.ch
www.karger.com

1015–9770/12/0334–0369$38.00/0

Accessible online at:
www.karger.com/ced

Masatoshi Koga, MD
Division of Stroke Care
National Cerebral and Cardiovascular Center
5-7-1 Fujishirodai, Suita, Osaka 565-8565 (Japan)
Tel. +81 6 6833 5012, E-Mail koga@hsp.ncvc.go.jp

digital subtraction angiography (DSA) [9, 10], magnetic resonance imaging (MRI) [11], magnetic resonance angiography (MRA) [12, 13], computed tomography angiography (CTA) [14–16] and conventional transsurface carotid ultrasonography (TSCU) [17–20], TSCU is handy and safe. However, ICA dissection typically occurs at least 2 cm distal to the bifurcation, at the level of the second and third cervical vertebrae, and extends over a variable distance [3]. The distal extracranial ICA cannot be examined by TSCU as it lies behind bones and cannot be imaged in B-mode. Doppler on TSCU can provide information about the distal ICA only if there is a flow-limiting stenosis or occlusion that results in abnormal waveforms. Thus, the lesion may be underdiagnosed by routine TSCU examination.

Transoral carotid ultrasonography (TOCU), a new ultrasound technique that was developed in our institute [21], can identify the distal extracranial ICA that is invisible on TSCU [21]. We and others have reported the utility of TOCU in evaluating various ICA pathologies, including distal extracranial ICA stenosis, occlusion, pseudo-occlusion, moya moya disease and dissection [22–28]. In particular, TOCU seems to be superior to TSCU in detecting ICA dissection during acute stroke because of its ability to visualize the high portion of the extracranial ICA. We previously reported some cases with ICA dissection proven by TOCU [26–28]. However, the utility of TOCU should be assessed not only in isolated cases. In this study, the utility of TOCU in evaluating consecutive patients with ICA dissection as the final diagnosis was examined based on comparison with other imaging modalities, such as DSA, MRI and TSCU.

Subjects and Methods

Patients with stroke or transient ischemic attack (TIA) caused by extracranial ICA dissection confirmed by DSA from our database of 6,026 patients with ischemic stroke or TIA who were admitted to our hospital between 1999 and 2010 were reviewed.

Basically, all patients in our database underwent intracranial MRI/MRA and TSCU unless MRI was contraindicated. When ICA stenosis or occlusion was detected on these regular examinations or when dissection was suspected as a cause of ICA lesions based on typical histories and symptoms, including sports activities and cephalocervical pain, or absence of other obvious causes for the lesions, DSA was performed after obtaining the patient's informed consent. Three-dimensional (3D) rotational angiography with a standard Integris BV5000 biplane system (Philips Medical System, Best, The Netherlands) was also performed if needed. The system provides contrast angiographic vascular luminal rotational X-ray image acquisition in multiple planes with reconstruction on a 3D work station [10]. The diagnosis of ICA dissection was made by DSA based on the review by Provenzale [11] and the criteria of the Spontaneous Cervicocephalic Arterial Dissections Study [29]. Briefly, the presence of an intimal flap with a double lumen was a direct finding for identifying ICA dissection. The pearl-and-string sign, string sign, pearl sign, retention of contrast, total occlusion with proximal distension, and tapered occlusion on DSA needed further evidence, such as morphological change on DSA or intramural hematoma on T_1 MRI. The level of the dissection was established based on DSA findings. The findings of TSCU, TOCU and MRI/MRA were compared using DSA as the gold standard. Patients' clinical backgrounds, stroke types, stroke risk factors, and prognoses were reviewed as well.

TSCU and TOCU Examinations

TSCU and TOCU examinations were performed using an ATL Ultramark 9 HDI (Advanced Technology Laboratories, Bothell, Wash., USA) with a 5- to 10-MHz linear probe and a 5- to 9-MHz micro convex probe, respectively, or an Aplio™ XU (Toshiba Co. Ltd, Tokyo, Japan) with a 7.5-MHz linear probe and a 6-MHz micro convex probe, respectively. For TSCU examination, the standard approach using B mode, color flow imaging, and pulsed Doppler was performed in the decubitus position. The probes for TOCU examination were originally designed for transrectal use. We performed TOCU in patients with ICA territory stroke who were suspected to have pathological lesions at the extracranial distal ICA based on TSCU or intracranial MRI/MRA findings; evaluation of the extracranial distal ICA was mandatory. We used a protocol for identifying patients who needed to undergo further evaluations for ICA dissection, notably patients with ICA territory ischemia or retinal ischemia of unknown etiology based on standard evaluations including head computed tomography, head MRI and MRA, TSCU, electrocardiogram monitoring and blood test. Those with concomitant symptoms or signs, such as headache, neck pain, face pain, ipsilateral Horner's syndrome, pulsatile tinnitus or lower cranial nerve palsy, were especially suspected of having ICA dissection. For such patients, DSA or cervical MRI/MRA was preferentially performed and TOCU was added if needed prior to mid-2008. After mid-2008, TOCU was preferentially performed. TOCU was repeated to evaluate morphological changes every 1–3 days during hospitalization when ICA dissection was detected on initial examination. The details of the TOCU examination procedure have been reported previously [21]. Briefly, the probe was covered with a disposable probe cover made of sterile thin gum after covering the tip of the probe with echo jelly. Then, the probe was inserted transorally and touched the pharyngeal posterolateral wall. Basically, we did not use local anesthesia because the pharyngeal reflex rarely occurs. For patients with severe pharyngeal reflex, one or two pushes of 8% xylocaine spray to the pharyngeal posterolateral wall were used. The display was in the vertical plane to longitudinally detect and assess extracranial ICA, and in the axial plane for horizontal assessment. The ICA was identified by delineation of a vessel running linearly from the lower to the upper pharynx and by confirming that flow was proceeding upward to the skull base and that branching was absent using B-mode and color flow imaging. The ICA was usually identified at the level of the second and third cervical vertebrae, based on our unpublished data, which show the spatial relationship between the TOCU probe and the cervical vertebrae on the X-ray. B-mode was used

Table 1. Clinical characteristics

	Case 1 [26]	Case 2 [28]	Case 3	Case 4 [27]	Case 5	Case 6	Case 7	Case 8
Sex	male	male	female	male	male	male	male	male
Age, years	37	52	62	69	51	57	42	48
Type of stroke	IS	TIA	IS	IS	IS	IS	IS	IS
Prior history of stroke	absent	absent	absent	absent	absent	absent	absent	absent
Risk factors	dyslipidemia, smoking, drinking	hypertension	none	none	none	none	hypertension	none
Affected side	right	right	right	left	right	left	right	left
Cephalocervical pain	headache	absent	absent	orbital pain	absent	absent	headache	headache
Neurological findings	hoarseness, hemiparesis	hemiparesis	dysarthria, hemiparesis	hyperesthesia, visual field blurring	USN, dysarthria, hemiparesis, hypoesthesia	aphasia	USN, dysarthria, hemiparesis, hypoesthesia	aphasia, hemiparesis

IS = Ischemic stroke; USN = unilateral spatial neglect.

to measure the distal ICA diameter from the near to the far adventitial edge. Pulsed Doppler was used to measure the flow velocity of the distal ICA with an angle correction within 60° between the blood flow direction and the Doppler interrogation. Color Doppler was used to identify flow signals in true and false lumens. The lumen which tapered from the ICA was defined as a true lumen and the other was defined as a false lumen [17]. When flow signals were absent in false lumens, the lumens were considered to be thrombosed. An intimal flap with a double lumen was a definite finding for identifying ICA dissection by both TSCU and TOCU. Furthermore, the maximum diameter of the dilated extracranial ICA was measured from the near to the far adventitial edges and compared with the diameter of the contralateral ICA at almost the same distance from the carotid bifurcation. The probe was carefully horizontally swept in the vertical plane to detect the maximum diameter of the vessel's center to avoid overmeasurement in case the vessel is tortuous or turning.

MR Examinations

MRI of the cervical ICA was performed on a 1.5-tesla scanner (Magnetom Vision or MAGNETOM Sonata, Siemens Medical Systems, Erlangen, Germany) with standard neck array coils. The MRI protocol was composed of T_1-weighted images and 3D-time of flight MRA. MRA was performed on both intracranial and extracranial vessels. Intracranial MRA was performed on admission and extracranial MRA was performed during hospitalization. Gadolinium-enhanced MRA was not performed routinely. Intramural hematoma and luminal diameter on both sides were assessed by T_1 MRI while intimal flap with double lumen, stenosis and dilatation, and pseudoaneurysm were evaluated by MRA by an experienced radiologist. Patients who did not tolerate MRI because of claustrophobia or because they had pacemakers were diagnosed based on brain CT and DSA.

Data Evaluation

Continuous variables were compared with the Wilcoxon signed rank test. A value of $p < 0.05$ was considered statistically significant.

Results

Eight patients (7 men, age 37–69 years) with extracranial ICA dissection were identified from the database. Seven patients developed ischemic stroke and 1 developed TIA ipsilaterally to the affected ICA. The initial TOCU examination was performed after confirmation of dissection by DSA in 5 patients and prior to DSA in the other 3 (cases 5, 6, 8), whose clinical history strongly suggested ICA dissection. The detailed clinical presentations of 3 of these 8 patients have been previously reported [26–28]. Table 1 summarizes the patients' clinical characteristics, and table 2 shows the results of the DSA, TSCU, TOCU and MRI/MRA examinations. The basis of the diagnosis by DSA was the double-lumen sign with an intimal flap in 2, dilatation and stenosis in 3, and tapered occlusion in 4. On DSA, the dissection site was restricted to the level between the first and third cervical vertebrae in 4 patients, and the dissection extended from the third cervical vertebra to the intracranial ICA in the remaining 4 patients. Four patients showed morphological changes of dissection on follow-up DSA. In case 2, who initially had an intimal flap with a double lumen on day 1, a saccular type pseudoaneurysm was detected on day 16. In case 4, who initially had severe stenosis on day 1, an intimal flap with a double lumen with a fusiform-type pseudoaneurysm appeared on day 7. In case 5, who initially had proximal dilatation and stenosis, and a distal saccular-type aneurysm on day 3, the stenotic lesion became wider and an additional aneurysm was detected on day 19. In case 8, who initially had an ICA tapering occlusion on day 1, the ICA was recanalized on day 17. Figures 1 and

Table 2. Imaging findings

Modality	Findings	Case 1 [26]	Case 2 [28]	Case 3	Case 4 [27]	Case 5	Case 6	Case 7	Case 8
CT/MRI	location of ischemia	ant-choroid, PCA	corona radiata	MCA cortex	MCA central gyrus	MCA cortex and deep area	MCA cortex	MCA cortex	MCA cortex
DSA	location of dissection	C3-siphon	C1–C2	C1–C2	C1–C2	C1–C3	C3-distal IC	C3-distal IC	C3-distal IC
	location of carotid artery bifurcation	between C3 and C4	C3	between C3 and C4	C3	between C3 and C4	C4	C4	between C3 and C4
	intimal flap with double lumen[1]	–	–	present	present	–	–	–	–
	dilatation and stenosis	–	present	–	present	present	–	–	–
	tapering occlusion	present	–	–	–	–	present	present	present
	pseudoaneurysm	–	saccular	fusiform	fusiform	saccular	–	–	–
	morphological change	–	present	–	present	present	–	–	present
TOCU	intimal flap/double lumen[1]	present	present	present	present	present	present	present	present
	false lumen	thrombosed	thrombosed	not thrombosed	thrombosed[2]	thrombosed	thrombosed	thrombosed	thrombosed[2]
	stenosis	–	present	–	present	present	–	–	–
	occlusion	–	–	–	–	–	–	–	–
	dissected arterial diameter, mm	7.1	7.3	6.3	7.0	7.9	6.5	7.7	6.5
	contralateral arterial diameter, mm	5.0	4.0	5.6	5.6	4.4	4.9	4.2	4.9
	pseudoaneurysm	–	undetectable	fusiform	fusiform	saccular	–	–	–
	morphological change	–	present	–	present	present	–	–	present
	initial Doppler flow abnormality	present[3]	present[4]	–	present[3]	–	present[3]	present[3]	present[3]
	sequential flow pattern change	–	present[2]	–	present[4]	present[4]	–	–	present[5]
TSCU	intimal flap/double lumen[1]	–	–	–	–	–	–	–	–
	arterial narrowing	present	–	–	–	present	–	–	present
	dissected arterial diameter, mm	8.8	9.9	4.3	6.7	5.8	4.5	4.8	8.5
	contralateral arterial diameter, mm	7.3	5.9	4.0	5.3	6.0	4.8	4.3	5.4
	arterial dilatation	–	present	–	–	–	–	–	–
	morphological change	–	–	–	–	present	–	–	present
	initial Doppler flow abnormality	present[3]	–	–	present[3]	–	present[3]	present[3]	present[3]
	sequential flow pattern change	–	–	–	present[5]	present[4]	–	–	present[5]
Cervical MRI and MRA	intimal flap with double lumen	–	–	present	present	–	–	–	–
	intramural hematoma	present	present	–	–	present	present	present	present
	ICA stenosis	–	present	–	–	present	–	–	present
	occlusion	present	–	–	–	–	present	present	present
	pseudoaneurysm	–	present	–	–	present	–	–	–

ant-choroid = Anterior choroidal artery; C1 = first cervical vertebra level; C2 = second cervical vertebra level; C3 = third cervical vertebra level; CT = computed tomography; MCA = middle cerebral artery; PCA = posterior cerebral artery; siphon, carotid siphon; USN = unilateral spatial neglect; C1–3 = cervical vertebra levels; siphon, carotid siphon.

[1] Direct findings of arterial dissection.

[2] Normalized peak flow velocity.

[3] Absence of end diastolic velocity indicating distal occlusion.

[4] High peak flow velocity (>200 cm/s) indicating stenosis.

[5] Normalized end-diastolic flow velocity.

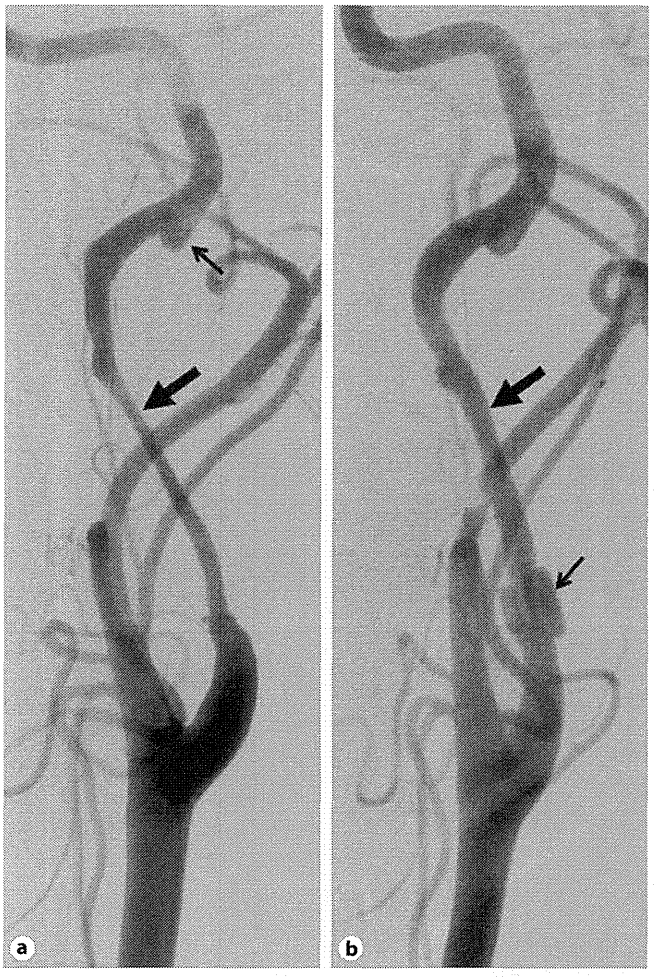

Fig. 1. Dissection of the extracranial ICA on a common carotid DSA image in case 5. **a** Right anterior oblique view on day 3. Dilatation and stenosis in the proximal ICA (thick arrow) and an aneurysm in the distal extracranial ICA (thin arrow) are shown. **b** Right anterior oblique view on day 19. The stenotic lesion becomes wider (thick arrow). A new aneurysm appears in the proximal ICA (thin arrow).

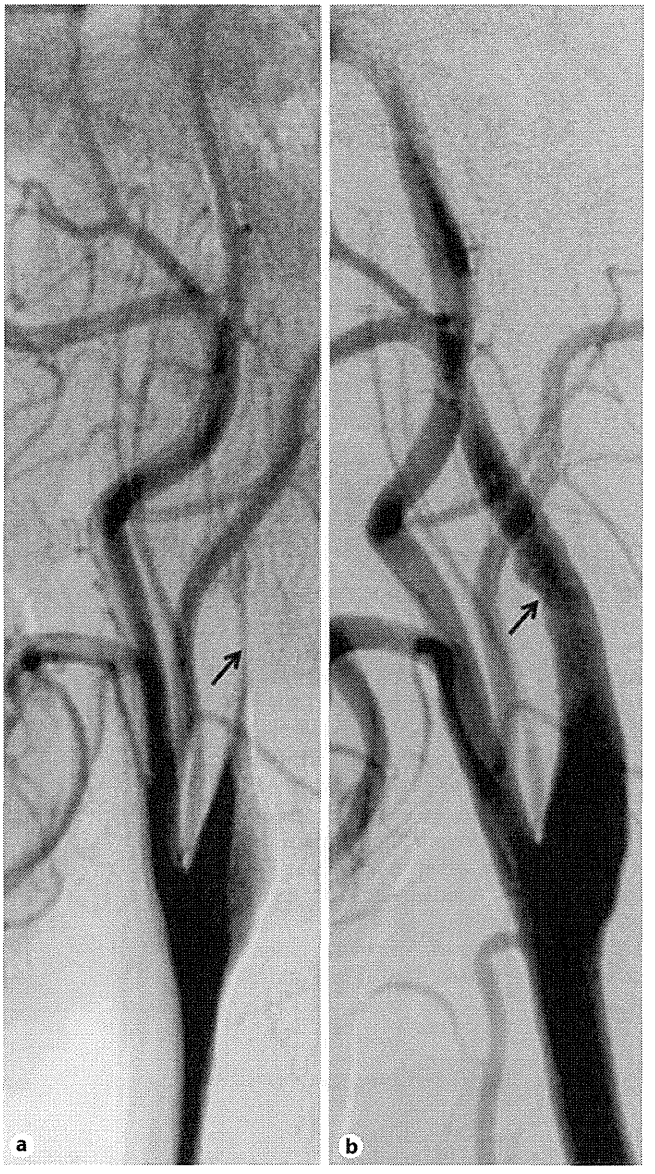

Fig. 2. Dissected ICA on a common carotid DSA image in case 8. **a** Lateral view on day 1, showing tapering ICA occlusion (arrow). **b** Recanalized dissected ICA (arrow) on day 17.

2 show sequential DSA images in cases 5 and 8, respectively.

By TOCU, a double lumen with an intimal flap was identified in all 8 patients. Color signals were absent in false lumens of 7 patients on the initial TOCU, indicating a thrombosed lumen; on the 2nd follow-up TOCU, little forward blood flow was present in the false lumen and in the course of time the flow volume increased gradually, indicating disappearance of the intraluminal thrombi in 1 patient (case 4) [27]. The luminal diameter at the height of the second cervical vertebra was 7.3 ± 0.7 mm in the dissected ICA and 4.9 ± 0.6 mm in the contralateral ICA in all patients ($p = 0.008$). No patient had a tortuous or turning vessel at the measurement point. On the initial Doppler examination, 5 patients displayed absence of end-diastolic velocity, indicating distal ICA occlusion, and 1 patient had ICA stenosis. As all the occluded arte-